In Vitro Phosphorylation of the Epidermal Growth Factor Receptor Autophosphorylation Domain by *c-src*: Identification of Phosphorylation Sites and *c-src* SH2 Domain Binding Sites

Christian R. Lombardo,[‡,§] Thomas G. Consler,[‡] and Daniel B. Kassel*[,§]

Departments of Protein Biochemistry and Bioanalytical and Structural Chemistry, Glaxo Wellcome, Inc., 5 Moore Drive, Research Triangle Park, North Carolina 27709

Received June 8, 1995; Revised Manuscript Received September 14, 1995[⊗]

ABSTRACT: During epidermal growth factor mediated signal transduction, intracellular receptor autophosphorylation on tyrosine residues results in the localization of several SH2 domain bearing proteins, including *c-src*, to the plasma membrane. This process is part of a complex pathway of specific protein associations that culminates in the regulation of cell growth and mitogenesis. The SH2 domain-mediated interaction of *c-src* with the EGF receptor has been demonstrated, yet the precise function of *c-src* in EGF receptor signaling remains unclear. The phosphorylation of EGFR by *c-src* was studied in order to evaluate the molecular basis for this interaction. The C-terminal autophosphorylation domain of EGFR was extensively phosphorylated by *c-src* and EGFR kinase activities *in vitro* as determined by electrospay ionization mass spectrometry. The sites of phosphorylation within the autophosphorylation domain (residues 976−1186) were identified by LC/MS, LC/MS/MS, and Edman sequencing. The majority of the sites identified corresponded to the known autophosphorylation sites of EGFR. Kinetic analyses of site-specific phosphorylation were made combining very fast enzyme digests (≤2 min) and high-speed, perfusion chromatography. These studies revealed that Y1086 was phosphorylated to a significantly higher extent by *c-src* than by EGFR. Additionally, Y1101 was identified as a unique *c-src* phosphorylation site. The function of these phosphorylation sites with respect SH2 domain interactions was investigated by affinity chromatography/mass spectrometry. A subset of peptides corresponding to the eight possible tyrosine phosphorylation sites within the EGFR autophosphorylation domain was demonstrated to bind to the SH2 domain of *c-src*. Those which bound to the SH2 domain included peptides derived from EGFR sequences flanking Y992, Y1086, Y1101, and Y1148. These data indicate that specific EGF receptor *c-src* phosphorylation sites are also ligands for the SH2 domain of *c-src*. Finally, extensive *c-src* phosphorylation of EGFR promoted its conversion to a form that exhibits high-affinity (K_D = 380 nM) and cooperative (Hill coefficient; n = 2) binding to the SH2 domain of *c-src* as measured by surface plasmon resonance. The identification of *c-src* phosphorylation sequences on EGFR as *c-src* SH2 binding sites supports the notion that this interaction plays a significant role in the regulation of growth factor receptor function and signal transduction.

The epidermal growth factor receptor (EGFR)[1] is a prototypic member of a family of receptor tyrosine kinases (Carter & Kung, 1994; van der Geer et al., 1994). Upon binding EGF, receptor autophosphorylation on tyrosine residues creates high-affinity interaction sites for several SH2 domain containing proteins including *c-src*, PLC-γ, grb2, and p85 regulatory subunit of PI3-kinase, shc, and GAP [reviewed in Fry et al. (1993) and Schlessinger (1994)]. These proteins act in concert to effect a signal transduction cascade ultimately responsible for the control and regulation of mitogenesis. The role of many of these protein interactions with EGFR is partially understood. The association of grb2 and shc is responsible for the activation of ras and downstream MAP kinase pathways (Lowenstein et al., 1992; Li et al., 1994). In contrast, the binding of GAP permits modulation of the ras-mediated signal transduction pathway (Ellis et al., 1990; Garrett et al., 1989; Setttleman et al., 1992). The association of PLC-γ results in its tyrosine phosphorylation by EGFR which permits complete PLC-γ activation (Rotin et al., 1992). Similarly, in the PI3-kinase pathway, p85 binding induces conformational changes that are transmitted to the p110 catalytic subunit, which increases its activity (Shoelson et al., 1993; Panayotou et al., 1992). The role of *c-src* binding to autophosphorylated EGFR (Luttrell et al., 1994) in EGFR-mediated signal transduction is less clear. Cell lines overexpressing *c-src* have increased EGF-induced mitogenesis (Luttrell et al., 1988) which requires myristylation, and active SH2 and kinase domains (Wilson et al., 1989). In addition, *v-src*-expressing cell lines have elevated levels of receptor phosphorylation (Wasilenko et al., 1991). These findings implicate *c-src* in the up-regulation of EGFR signaling.

* To whom correspondence should be addressed. Telephone: 619-453-6027. Fax: 619-453-4426. E-mail: dkassel@adnc.com.

‡ Department of Protein Biochemistry.

§ Department of Bioanalytical and Structural Chemistry.

⊗ Abstract published in *Advance ACS Abstracts,* November 15, 1995.

[1] Abbreviations: EGFR, epidermal growth factor receptor; EGFR-KD, epidermal growth factor receptor-kinase domain; LC/MS, liquid chromatography/mass spectrometry; TIC, total ion current chromatogram; DTT, dithiothreitol; SH2, src homology 2; BAD, biotin attachment domain; BSA, bovine serum albumin; HEPES, *N*-(2-hydroxyethyl)-piperazine-*N*′-2-ethanesulfonic acid; PCR, polymerase chain reaction; SDS−PAGE, sodium dodecyl sulfate−polyacrylamide gel electrophoresis; EDTA, ethylenediaminetetraacetic acid; EGTA, ethylene glycol bis(β-aminoethyl ether)-*N*,*N*,*N*′,*N*′-tetraacetic acid; PMSF, phenylmethanesulfonyl fluoride.

0006-2960/95/0434-16456$09.00/0

Although *c-src* is known to associate with phosphorylated EGFR *in vitro*, the molecular details of this interaction are not well understood. EGFR is an *in vitro* substrate for the tyrosine kinase activity of *c-src*, but the sites of phosphorylation have not been completely characterized (Koland et al., 1990). As a first step toward assessing the molecular basis of the *c-src*-EGFR interaction, the *in vitro* sites of *c-src* phosphorylation within the autophosphorylation domain of EGFR have been identified. Using the recombinant EGFR autophosphorylation domain as a model system, liquid chromatography/electrospray ionization methods have been developed to map multiple phosphorylation sites. Rapid enzyme digestions on immobilized trypsin perfusion columns and fast HPLC (perfusion chromatography) tryptic mapping coupled with LC/MS, LC/MS/MS, and Edman sequencing have allowed a semi-quantitative comparison of the kinetics of site-specific phosphorylation within EGFR. The peptide sequences containing phosphotyrosine within the EGFR autophosphorylation domain that interact with the SH2 domain of *c-src* have been determined by affinity chromatography/HPLC/MS. Furthermore, extensive *c-src* phosphorylation of the EGFR autophosphorylation domain is demonstrated, by surface plasmon resonance (BIAcore), to promote its conversion to a form that exhibits high-affinity and cooperative binding to the SH2 domain of *c-src*. The conclusions from these model studies are that the sites of *c-src* phosphorylation also represent sequences on EGFR that preferentially associate with the SH2 domain of *c-src*. The results support the concept that the substrates of tyrosine kinases preferentially associate with SH2 domains found within these same kinases (Songyang et al., 1995; Mayer et al., 1995). Collectively, these findings suggest that specific *c-src*−EGFR interactions are an important component of the signal transduction cascades.

MATERIALS AND METHODS

Materials. Phenyl-Sepharose chromatography medium was from Pharmacia. Poros R2/H, Poros HQ, Poros S, and Poroszyme were from PerSeptive Biosystems. HEPES was from U.S. Biochemical Corp. The intracellular tyrosine kinase domain of EGFR (EGFR-KD) was obtained from Stratagene. *c-src* containing the tyrosine kinase domain was purified from baculovirus-infected SF9 cells as described (Ellis et al., 1994). All other chemicals were obtained from Sigma.

EGFR Autophosphorylation Domain and c-src SH2 Domain Cloning, Expression, and Protein Purification. The autophosphorylation domain of human EGFR (amino acids 976−1186) was expressed with an N-terminal Glu-Glu epitope sequence tag, MEYMPE, using a modified pET16B in *Escherichia coli* strain BL21(DE3) under the control of the T7 promoter (K. Lewis and I. Patel, unpublished results). The EGFR autophosphorylation domain was purified from *E. coli* lysates on a 2.6 × 2.5 cm Poros HQ column equilibrated with 20 mM HEPES, 1 mM EDTA, and 1 mM DTT, pH 6.5, and eluted with a linear gradient of 0−400 mM NaCl. Fractions containing the autophosphorylation domain were pooled, adjusted to 1.5 M NaCl, and loaded onto a 1.6 × 50 cm phenyl-Sepharose fast flow column. The flow-through fraction was collected and precipitated with $(NH_4)_2SO_4$ at 25% saturation. The pellet containing the EGFR autophosphorylation domain was resuspended and was greater than 95% pure.

The SH2 domain of *c-src* (residues 144−249) was prepared as a fusion protein with the biotin attachment domain from the α-subunit of oxalacetate decarboxylase from *Klebsiella pneumoniae*. This fusion protein is biotinylated *in vivo* during expression at a unique site in the decarboxylase domain. A *Sal*I site was introduced at the 3′ end of the gene encoding the *c-src* SH2 domain, allowing for the in-frame insertion of a DNA fragment encoding the biotin attachment domain (BAD), which is flanked by *Sal*I sites. Ligation products were screened for correct insertional orientation, yielding hybrid plasmid pUSH2/BAD. This chimeric gene was subcloned as an *Nde*I/*Bam*HI fragment into pET11b. The SH2−BAD protein was purified to 95% from *E. coli* strain BL21(DE3) lysates in 20 mM HEPES, 5 mM EDTA, and 5 mM DTT, pH 8, using a Poros S column eluted with a linear gradient of NaCl.

Phosphorylation Reactions. In vitro conditions for the phosphorylation of the EGFR autophosphorylation domain were 15 μM EGFR protein, 20 mM HEPES, 10 mM $MgCl_2$ (*c-src*) or 10 mM $MnCl_2$ (EGFR-KD), 18 μg/mL kinase, 100 μM Na_3VO_4, 1 mM ATP, 1 M $(NH_4)_2SO_4$, and 10 μg/mL each of leupeptin, aprotinin, and phenylmethanesulfonyl fluoride, pH 7.4 (Wedegaertner & Gill, 1989). Phosphorylations were initiated by addition of ATP for 2 min followed by addition of the EGFR autophosphorylation domain. Time points were taken to follow the course of the phosphorylation reaction, as indicated in the figure legends. All reactions were performed at 37 °C and were quenched with a final concentration of 100 mM EDTA. All kinetic data were analyzed by nonlinear regression assuming simple first-order kinetics, with the equation: % phosphorylation = (% phosphorylation$_{max}$)$(1 - e^{-kt})$. The first-order rate constant (k) obtained from these analyses was expressed as a half-life ($T_{1/2}$) using the relationship: $T_{1/2} = \ln 2/k$.

Liquid Chromatography/Mass Spectrometry. Electrospray ionization mass spectrometry (ESI-MS) was performed on a Sciex API III triple quadrupole mass analyzer (PE-Sciex, Thornhill, Ontario, Canada) interfaced with a Hewlett Packard 1090 microbore liquid chromatograph. Buffer conditions were as follows: buffer A contained 0.05% TFA in water, and buffer B contained 0.045% TFA in 9:1 acetonitrile/water. For protein analyses, a Poros R2/H 250 μm × 40 cm capillary perfusion column was used. Aliquots of the phosphorylation reactions (corresponding to 100 pmol) were injected onto the column and eluted into the mass spectrometer ion source using a gradient of 15−65% buffer B in 5 min.

Protein Molecular Weight Determinations. Protein molecular weights were generated by scanning the quadrupole from 930 to 1080 Da in 3 s using a 0.2 Da step and 4.0 ms dwell time. The resolution of the instrument was 1500 (10% valley definition), and the orifice potential was set to 80 V for all protein analyses. It was found previously that ion intensities of individual phosphorylated species by electrospray ionization mass spectrometry accurately represent the "true" molar ratios of the phospho isoforms (Lenhard et al., 1995). Thus, the amount of phosphate incorporation into the EGFR autophosphorylation domain could be derived from the electrospray mass spectra using the equation:

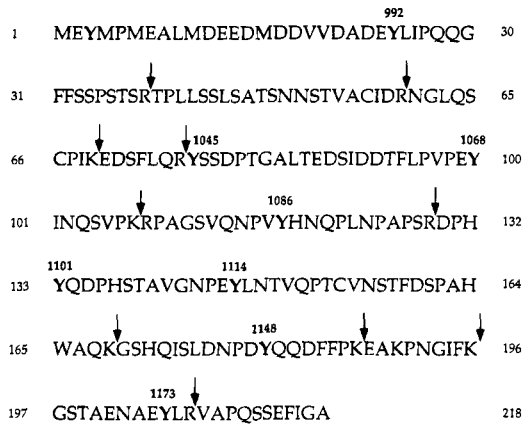

FIGURE 1: Amino acid sequence, tryptic cleavage sites, and tyrosine phosphorylated residues of the recombinant EGFR autophosphorylation domain. Shown is the recombinant EGFR autophosphorylation domain sequence with the residues numbered. The sites of tryptic cleavage are designated by a vertical arrow. The tyrosine residues are bolded, and their sequence position within the native, full-length EGFR is indicated.

$$\text{mol of phosphate incorporated} = i[I_i/\sum_{i=0}^{n} I_i]T$$

where i = the phosphorylation state, I_i = the mass spectrometric integrated area for the phosphorylated species i, n = the number of phosphate moieties, and T = total moles of protein being analyzed.

Phosphorylation Site Tryptic Mapping and Identification. Proteolytic cleavage of each of the phosphorylated protein time points was achieved rapidly (≤2 min) utilizing an immobilized trypsin perfusion column (PerSeptive Biosystems, Framingham, MA). The calculated masses and corresponding EGFR tyrosine phosphorylation site(s) of the tryptic peptides are summarized in Table 1. The amino acid sequence of the recombinant EGFR autophosphorylation domain, the location of tryptic cleavage sites, and identified tyrosine phosphorylation sites are designated in Figure 1. Aliquots corresponding to 200 pmol of the phosphorylation reactions were quenched with EDTA and injected directly onto a custom-packed PEEK 500 μm × 15 cm immobilized trypsin perfusion (Porosyme) column equilibrated in 50 mM NH_4HCO_3 (pH 8.5). The immobilized enzyme column was placed in a column heater compartment and maintained at a temperature of 37 °C for all digestions. Phosphorylated protein samples were injected onto the Poroszyme column at a flow rate of 20 μL/min, corresponding to a column residence time of 1.5 min. Digestion products were collected into an Eppendorf tube, and aliquots corresponding to 25−50 pmol were analyzed by LC/MS using a 300 μm × 15 cm capillary Hypersil C18 reverse-phase column (LC Packings, USA, San Francisco, CA). Peptides were separated using a gradient of 5−55% buffer B in 25 min. The mass spectrometer was scanned from 400 to 1900 Da in 3 s using a 0.5 Da step and a 1.0 ms dwell time. The orifice potential was 80 V, and the ion multiplier was set to −3900 V. The instrument resolution was set to 1000 (10% valley definition) using a standard PPG calibrant solution. Calibration spectra were acquired by direct infusion of the calibrant solution into the mass spectrometer at a flow rate of 5 μL/min and recorded using a 0.1 Da step size.

Phosphorylated peptides were identified readily by one of two methods. In the majority of cases, it was possible to identify the phosphorylated tryptic peptides based on the appearance of a peptide whose mass shifted from the predicted peptide mass by 80 Da (*i.e.*, the mass of phosphate group). Unequivocal identification of phosphorylated tryptic peptides was achieved using the "stepped orifice potential" technique (Huddleston et al., 1993; Ding et al., 1994). Briefly, this technique involves analyzing the peptide digest in the negative ion mode and varying the voltage difference between the ion entrance aperture and the skimmer so that an eluting peptide can be caused to undergo partial fragmentation. Within the orifice/skimmer region of the mass spectrometer, ions undergo collision-induced dissociation. As the voltage difference between the orifice and skimmer elements increases, the energy of the collisions between intact peptide ions and the gas molecules within this orifice/skimmer region increases. Tyrosine phosphate bonds are readily cleaved when a high potential difference (250 V) is applied to these two elements. In the negative ion mode, consequently, the PO_3^- anion is readily detected. This ion is diagnostic for phosphorylation [see Huddleston et al. (1993) and Ding et al. (1994)]. By scanning (or "stepping") the orifice voltage as a function of the *m/z* ratio, molecular anions, $(M-H)^-$, and phosphate, PO_3^-, anions are detected. For these experiments, an identical aliquot of sample was analyzed in the negative ion mode. The mass spectrometer was scanned from 75 to 1825 Da in 3.7 s using a 0.5 Da step and a 1.0 ms dwell time. The orifice potential (OR) was "stepped" as follows: OR = −250 V over the mass range *m/z* 75−525, OR = −100 V for *m/z* 525−1125, and OR = −140 V for *m/z* 1125−1825. Phosphopeptides were rapidly identified by the appearance of an abundant ion at *m/z* 79, corresponding to PO_3^-. The ratio of phosphorylated to nonphosphorylated tryptic peptide was obtained by integrating the areas over the peaks of interest in the total ion current chromatograms.

Phosphorylation site identification in tryptic peptides containing two tyrosines was achieved by LC/MS/MS analysis and/or Edman sequencing. In the LC/MS/MS method, the phosphorylated peptide of interest is selected in the first stage of the mass spectrometer and dissociated by collision with a neutral gas in the second stage of the mass spectrometer, and the products of this collision-induced dissociation are analyzed in the third stage of the triple quadrupole mass spectrometer. Depending on the mass (and charge state) of the precursor ion, a collision energy of either 25 or 35 eV was used. The collision gas was Ar/N_2, and the collision gas pressure was roughly 190 collison gas thickness (cgt) units (*ca.* 1.9×10^{14} atoms/cm^2). The precursor ion mass resolution was degraded to 300 (10% valley definition) in order to increase signal-to-noise. Product ion resolution was set to approximately 500 (10% valley definition). The size of some of the tryptic peptides containing multiple tyrosine residues precluded their sequencing by mass spectrometry. Consequently, these tryptic peptides were HPLC-purified and subjected to N-terminal Edman sequencing. In some cases, a secondary digestion of these HPLC-purified tryptic peptides was performed with Asp-N (overnight at 37 °C). These digest products were analyzed by LC/MS and/or LC/MS/MS, as described above.

Integral Microanalytical Workstation. An Integral microanalytical workstation (PerSeptive Biosystems) was used

for SH2−EGFR peptide binding studies. The workstation consists of three 10-port injector valves and was configured for two-dimensional separations coupled with mass spectrometry as described previously (Kassel et al., 1995). The first dimension of the 2-D chromatographic system consisted of a custom-packed SH2 affinity column. The affinity column was prepared by preincubating several nanomoles of purified SH2−BAD with 100 μL of bulk streptavidin Poros resin and slurr-packing into 750 μm × 5 cm PEEK tubing equipped with a 0.062 × 0.025 in. stainless-steel frit (Mott Metallurgical) at the outlet of the column. The second dimension of the 2-D chromatographic system consisted of a reverse-phase Poros R2/H 250 μm × 20 cm PEEK packed column. The SH2−BAD affinity column was stored in a temperature-controlled column heating/cooling compartment at 5 °C and equilibrated in binding buffer (20 mM Tris, 150 mM NaCl, 2 mM EDTA, and 1 mM DTT, pH 7.4). An eight-component synthetic EGFR phosphopeptide mixture containing each of the eight putative EGFR autophosphorylation sites was used for these studies, as described previously (Luttrell et al., 1994). A 10 μM aliquot corresponding to 200 pmol of this peptide mixture was injected onto the affinity column and maintained on-column for 10 min. The column was then washed rapidly with 10 column volumes of binding buffer. Unbound (or weakly associated) peptides were trapped at the head of the reverse-phase Poros R2/H column and eluted into the ion source of the mass spectrometer using a gradient of 1−29% buffer B in 15 min. Phosphopeptides bound to the SH2−BAD affinity column were displaced by competition with 2 nmol of Ac-Y*EEIE peptide. The displaced peptides were trapped onto the reverse-phase column and analyzed by LC/MS in an analogous manner.

Surface Plasmon Resonance−BIAcore. Surface plasmon resonance (BIAcore) was utilized to measure binding interactions in real time. This technique of detecting protein−protein interactions is fully described in several recent publications (Chaiken et al., 1991; Panayotou et al., 1992; Zhou et al., 1993). The SH2−BAD was immobilized to an avidin-coated SA5 chip via the biotin moiety of the BAD fusion protein. The *c-src*-phosphorylated EGFR autophosphorylation domain was injected onto the SH2−BAD surface and the subsequent binding measured as an increase in resonance units (RU). The measured rates of association and dissociation were extremely rapid, which is consistent with other reports of phosphopeptide−SH2 interactions (Felder et al., 1993). Thus, the values of RU bound were taken at steady-state conditions. Controls for nonspecific binding were obtained by measuring the binding to the avidin surface alone at each concentration of phosphorylated EGFR tested. These controls for nonspecific binding were subtracted. In addition, nonphosphorylated EGFR autophosphorylation domain did not bind to the SH2−BAD surface. The dissociation constant, K_D, and Hill coefficient were determined by nonlinear regression analysis of the binding isotherms.

RESULTS

The C-Terminal Autophosphorylation Domain of EGFR Is a Substrate for c-src. The bacterially expressed autophosphorylation domain of the EGFR receptor, containing the known autophosphorylation sites but lacking the kinase domain, was chosen for these studies. Previous limited proteolysis studies of the intracellular region of EGFR have provided evidence that the tyrosine kinase domain and the C-terminal autophosphorylation domain are independently folded and separable regions (Gregoriou et al., 1994). The advantage of this approach is that the protein is not phosphorylated during expression in *E. coli*. An additional benefit to studying the isolated autophosphorylation domain is that there is no competing tyrosine kinase activity from the EGFR kinase domain. Consequently, the purified protein can be phosphorylated *in vitro* under defined conditions with *c-src* and the sites of tyrosine phosphorylation mapped. The functional consequences of phosphorylation with respect to interactions with the *c-src* SH2 domain can be characterized.

Figure 2 shows the molecular weight *vs* intensity plot (*i.e.*, deconvolution mass spectrum) of the nonphosphorylated EGFR-KD and *c-src*-phosphorylated EGFR autophosphorylation domain. LC/MS analysis of the purified EGFR autophosphorylation domain gave an average molecular mass of 24 054.7 Da ± 2.2 (SD) (calculated M_r = 24 053.4), indicating that no phosphorylation had occurred during expression (Figure 2A). Incubation of the autophosphorylation domain with catalytic amounts of *c-src* led to the disappearance of the nonphosphorylated form and the appearance of several new forms of the protein. The masses of these species were incrementally larger than the molecular species in Figure 2A by 80 Da, indicative of the addition of multiple phosphate moieties to the autophosphorylation domain (Figure 2C). Each of the peaks in the deconvoluted mass spectrum of Figure 2C refers to a specific phosphorylated species of the autophosphorylation domain (*i.e.*, di-, tri-, tetra-, and pentaphosphorylated, as designated in Figure 2C). For comparison, incubation of the autophosphorylation domain with exogenous EGFR-KD was performed under identical conditions. A similar incremental 80 Da mass increase was observed upon incubation of the autophosphorylation domain with EGFR-KD (Figure 2B). Western blotting with anti-phosphotyrosine antibodies confirmed that the phosphorylation by both kinases occurred on tyrosine residues (data not shown).

Time-course phosphorylation reactions allowed for a semiquantitative measure of the relative amount of phosphate incorporated into the autophosphorylation domain. This was accomplished by calculating the percentage of each of the phosphorylated species in the electrospray mass spectrum as described under Materials and Methods. Phosphorylation levels catalyzed by *c-src* approached a maximum of 4.1 mol of phosphate per mole of protein with $T_{1/2}$ = 16.4 min. In contrast, EGFR-KD incorporated a maximum of 3.7 mol of phosphate per mole of protein with $T_{1/2}$ = 36 min (Figure 3). These data demonstrate that the autophosphorylation domain of EGFR is a substrate for *c-src in vitro*.

Mapping the in Vitro c-src and EGFR Phosphorylation Sites on the EGFR Autophosphorylation Domain. To characterize the *c-src* tyrosine kinase activity toward the EGFR autophosphorylation domain, the sites of phosphorylation were mapped. The sites of phosphorylation by EGFR-KD were also identified, allowing for a direct comparison with the *c-src* sites. Samples of the EGFR autophosphorylation domain taken at the time points described in Figure 3 were subjected to rapid tryptic digestion

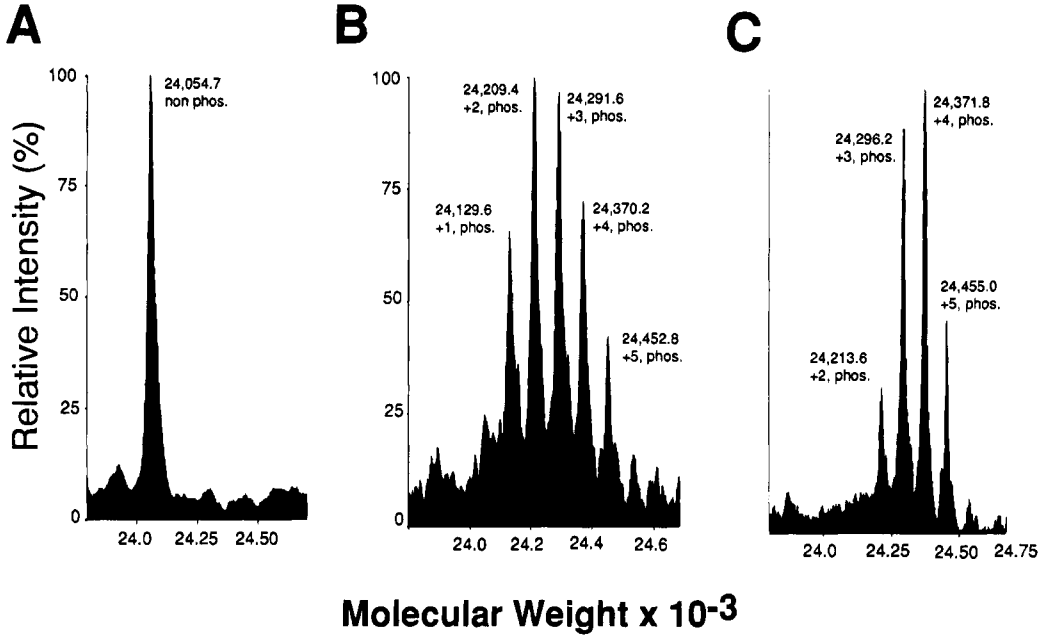

FIGURE 2: Purified EGFR autophosphorylation domain is a substrate for *c-src* and EGFR-KD activities *in vitro*. LC/MS of the EGFR protein was performed as described under Materials and Methods. Shown are the deconvoluted mass spectra of the purified EGFR C-terminal (A) without prior incubation with tyrosine kinases, (B) after incubation with EGFR-KD, and (C) after incubation with *c-src* for 60 min.

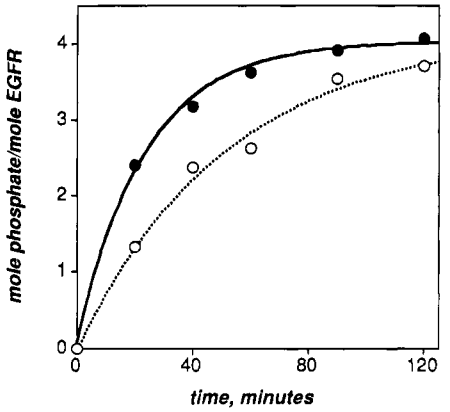

FIGURE 3: Kinetics of phosphate incorporation into the EGFR autophosphorylation domain. The relative amounts of phosphate incorporated into the EGFR autophosphorylation domain by *c-src* (●) or EGFR-KD (○) were calculated as described under Materials and Methods.

Table 1: Tryptic Peptides of the EGFR Autophosphorylation Domain

peptide	residues	calcd masses (Da)	phosphorylation site(s)
T1	1−39	4522.0	Glu-Glu tag, Y992
T2	40−60	2151.4	
T3	61−69	960.1	
T4	70−76	895.0	
T5	77−107	3400.7	Y1045, Y1068
T6	108−129	2400.7	Y1086
T7	130−168	4354.7	Y1101, Y1114
T8	169−187	2237.4	Y1148
T9	188−196	1004.2	
T10	197−207	1211.3	Y1173
T11	208−218	1106.2	

and analysis by LC/MS. The phosphorylation sites were identified based on unique mass fingerprints of the tryptic peptides (Figure 1, Table 1) and the ability to "extract" these ions from the total ion current chromatograms. Shown in Table 1 are the expected masses of the tryptic fragments for

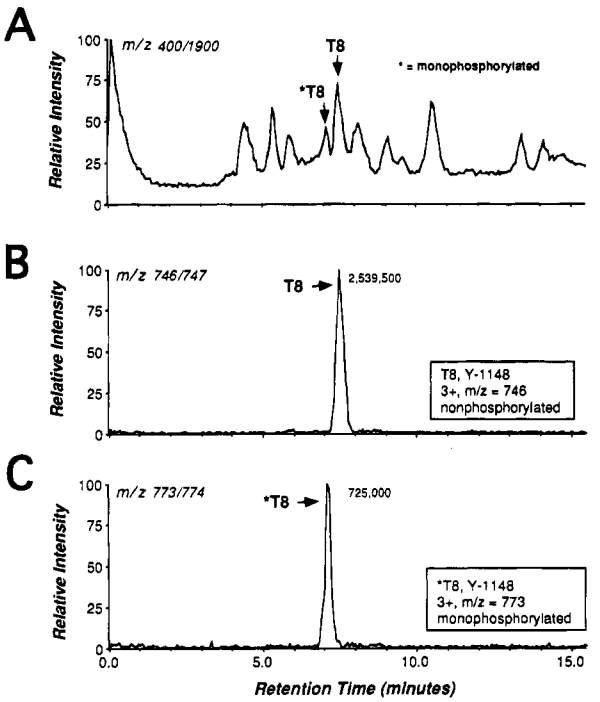

FIGURE 4: Tryptic phosphopeptide mapping of EGFR phosphorylation sites. EGFR phosphorylated by *c-src* for 90 min was digested with immobilized trypsin, and analyzed by LC/MS. (A) Representative TIC trace from LC/MS analysis (positive ion mode). (B) Mass chromatogram of T8 trypic peptide containing Y1148. (C) Mass chromatogram of the phosphorylated T8 tryptic peptide. The chromatograms in (B) and (C) represent the triply protonated $(M+3H)^{3+}$ form of the T8 peptide. The mass range scanned is shown in the upper left of the TIC. The integrated ion current is shown next to the apex of the peak in (B) and (C).

the EGFR autophosphorylation domain. A representative TIC is shown in Figure 4A for phosphorylation of the EGFR autophosphorylation domain by *c-src* for 90 min. The individual mass chromatograms for the nonphosphorylated and phosphorylated T8 tryptic peptide (corresponding to Y1148) are shown in Figure 4B and 4C, respectively. The

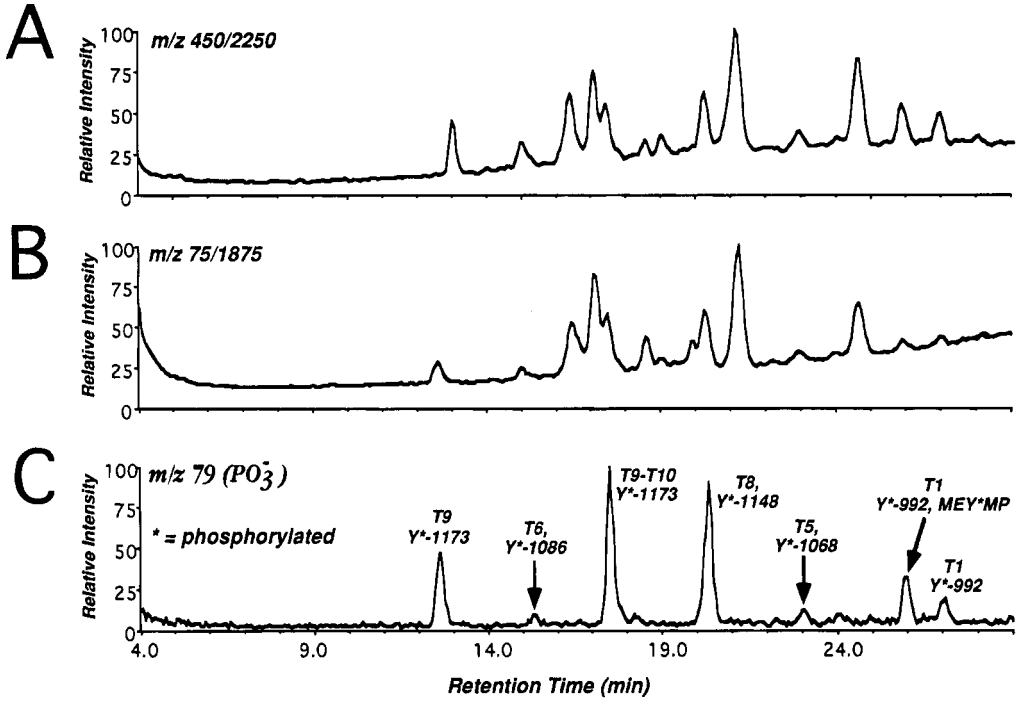

FIGURE 5: Identification of EGFR phosphorylation sites by negative ion orifice potential stepping. EGFR phosphorylated by *c-src* for 90 min was digested with immobilized trypsin, and analyzed by LC/MS using the stepped orifice potential technique described under Materials and Methods. (A) Positive ion TIC. (B) Negative ion TIC. (C) *m/z* 79, PO_3^- TIC. Shown in (C) are the peaks corresponding to identified EGFR phosphorylation sites.

chromatograms in Figure 4B,C represent the triply protonated $(M+3H)^{3+}$ form of the T8 peptide (*m/z* = 746 and 773 for the nonphosphorylated and phosphorylated forms, respectively). An identical procedure was used to determine the amount of phosphorylation present for each tryptic peptide, at a given time point (see below) by both *c-src* and EGFR-KD kinases. This analysis directly identified Y1086, Y1148, and Y1173 of the EGFR autophosphorylation domain as *c-src* phosphorylation sites (Table 2).

The stepped orifice potential technique (Huddleston et al., 1993; Ding et al., 1994) was used to confirm the phosphotryptic peptides identified from the mass fingerprint approach. Tryptic peptides were separated on a capillary Hypersil C18 column and analyzed by LC/MS in the negative ion mode. Phosphorylated tryptic peptides were detected by monitoring for the presence of *m/z* = 79 (corresponding to PO_3^- ion) by inducing fragmentation of the peptide with high voltage in the high-pressure region between the entrance orifice of the mass spectrometer and the skimmer. Shown in Figure 5B is the TIC chromatogram corresponding to the detection of the tryptic peptides for the 90 min phosphorylation reaction of the EGFR autophosphorylation domain with *c-src* in the negative ion mode. Figure 5C shows the mass chromatogram for *m/z* = 79 (corresponding to PO_3^-) from the same analysis. From this experiment, the phosphotryptic peptides were readily identified.

LC/MS/MS studies were performed on the phosphotryptic peptides (identified in the stepped orifice potential experiments) to confirm the phosphorylation site assignments. The predominant fragment ions were "b" and "y" ion series, arising from bond cleavage between the amide bonds of the peptide backbone (Biemann, 1990). Shown in Figure 6 is the product ion spectrum of the doubly protonated $(M+2H)^{2+}$ ion, corresponding to *m/z* 606.7 for the T10 peptide containing Y1173. A prominent C-terminal "y" ion series was observed. The mass difference between the y2 and y3 ions was 243 Da, corresponding to the residue mass of phosphotyrosine. From this product ion spectrum, the site of phosphorylation was readily determined. Phosphotryptic peptides were identified readily using both these techniques and corroborated the results of the mass fingerprint method.

Three tryptic peptides of the EGFR autophosphorylation domain contained two potential tyrosine phosphorylation sites: T1 (containing the sequence MEYMPME from the Glu-Glu epitope and EGFR site Y992), T5 (EGFR sites Y1045 and Y1068), and T7 (EGFR sites Y1101 and Y1114; Figure 1, Table 1). These peptides were further studied to resolve the sites of phosphorylation. The non-, mono-, and diphosphorylated forms of tryptic peptide T1 were observed in the LC/MS analysis. Each was purified by reverse-phase HPLC and subjected to N-terminal Edman sequencing. Y992 was identified as the major phosphate acceptor while phosphorylation of the Glu-Glu tag sequence-containing tyrosine residue was observed to a lesser extent. In contrast, only the non- and monophosphorylated forms of tryptic peptide T5 were observed. The monophosphorylated isoform of the T5 peptide was purified by reverse-phase HPLC and N-terminally sequenced. Sequence analysis demonstrated that Y1045 was unmodified, suggesting that Y1068 is the residue that is phosphorylated. Tryptic peptide T7 (putative sites Y1101 and Y1114) was similarly purified by HPLC and digested with Asp-N. The products of the T7 peptide Asp-N digest were analyzed by LC/MS as described previously. Modest phosphorylation of Y1101 (8%) was detected with *c-src* whereas no labeling of this residue was observed with EGFR-KD. It was not possible to detect a peptide containing the Y1114 site in any of the experiments performed. The sites and magnitude of phosphorylation by both kinases are summarized in Table 2. These data demonstrate that the sites of phosphorylation by both EGFR

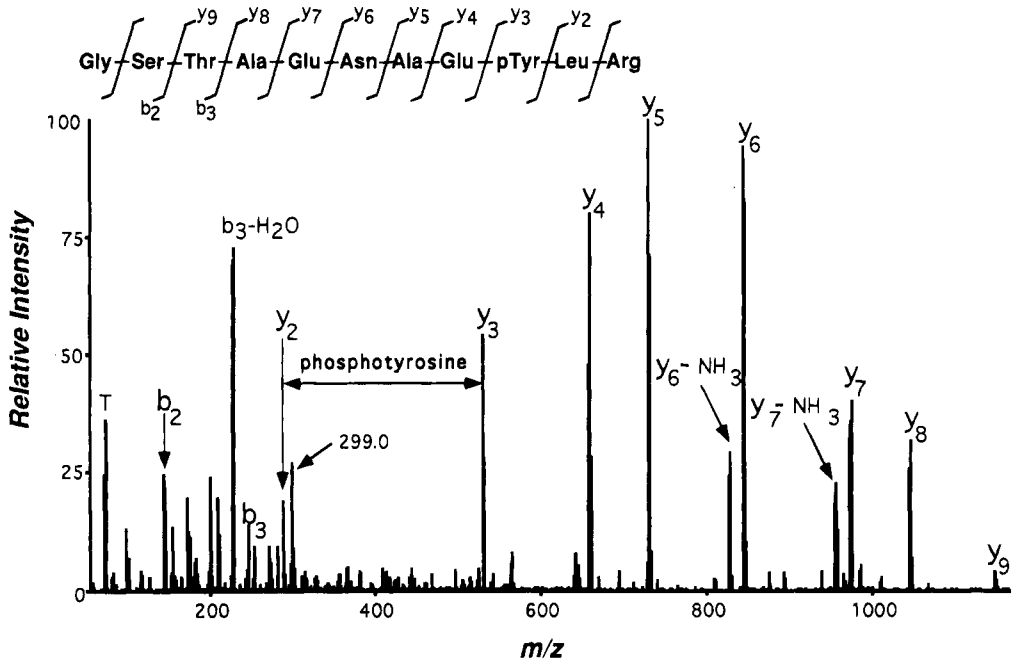

FIGURE 6: LC/MS/MS identification of Y1173 phosphorylation site. Shown is the LC/MS/MS spectrum obtained for peptide T10 containing Y1173. The mass difference between the C-terminal y_2 and y_3 ions corresponds to the residue mass of phosphotyrosine (243 Da) and is designated in the amino acid sequence of the T10 peptide.

Table 2: Summary of EGFR Phosphorylation Site and SH2 Domain Binding Data

P-Tyr site	sequence	*c-src* (%)	EGFR (%)	*c-src* SH2 binding
Y992	...DADEYLIPQQ...	46	46	yes
Y1045	...FLQRYSSDPT...	0	0	no
Y1068	...PVPEYINQSV...	11	30	no
Y1086	...QNPVYHNQP...	64	15	yes
Y1101	...RDPHYQDPH...	8	0	yes
Y1114	...GNPEYLNTV...	nd	nd	no
Y1148	...DNPDYQQDF...	26	41	yes
Y1173	...ENAEYLRVA...	67	66	no

and *c-src* are qualitatively similar. With the exception of Y1101, the majority of these sites correspond to the known autophosphorylation sites of EGFR: Y992, Y1068, Y1086, Y1143, and Y1173 (Downward et al., 1984; Hsuan et al., 1989).

Tyrosine Y1086 Is Extensively Phosphorylated by c-src. The results of the mapping experiments demonstrate that the sites of phosphorylation by *c-src* and EGFR-KD are similar and correspond to the known autophosphorylation sites of EGFR. Quantitative differences were observed in the overall amount of phosphate incorporated into the tyrosine residues as revealed by kinetic analysis of site-specific phosphorylation. Samples were taken at specific time points during the kinase reactions and injected directly onto the Poroszyme-immobilized trypsin column, and the products of these 1.5 min digestions were then analyzed by LC/MS. The sites of phosphorylation by both *c-src* and EGFR tyrosine kinase activities were mapped and levels of phosphorylation quantitated by integration of the areas in the extracted TIC chromatograms. Y992, Y1086, and Y1173 were phosphorylated most rapidly and extensively by *c-src* (Figure 7). Significantly, phosphorylation at Y1086 was 4 times higher by *c-src* than by EGFR-KD (Figure 7). Like *c-src*, EGFR-KD also phosphorylated Y992 and Y1173, extensively. EGFR-KD phosphorylated slightly higher levels at Y1068 and Y1148 than *c-src* (Figure 7). Thus, the major difference between *c-src* and EGFR-KD activities toward the EGFR autophosphorylation domain is that *c-src* phosphorylated Y1086 to a much greater level than EGFR-KD under identical conditions.

Specific EGFR Phosphopeptides Bind to the SH2 Domain of c-src. A potential consequence of EGFR phosphorylation by *c-src* is the availability of phosphotyrosine binding sites for the SH2 domains of signaling proteins. The question of whether EGFR sites that are phosphorylated by *c-src* also directly interact with the SH2 domain of *c-src* was addressed. The determinants for sequence-specificity of binding to SH2 domains are limited to 1−5 amino acids N- and C-terminal to the tyrosine residue (Songyang et al., 1993, 1994; Cantley & Songyang, 1994). Synthetic phosphopeptides derived from the eight possible tyrosine phosphorylation sites within the EGFR autophosphorylation domain (Figure 1) were examined for their ability to bind directly to the SH2 domain of *c-src*. These peptides are 13-mers and contain the phosphotyrosine residue (bolded in Figure 1) flanked by six amino acids N- and C-terminal. A TIC of an equimolar mixture of the eight phosphopeptides is shown in Figure 8A. An identical aliquot of the phosphopeptide mixture was loaded onto a *c-src* SH2 domain affinity column. Nonbinding phosphopeptides were trapped onto a Poros R2/H reverse-phase column and subsequently analyzed by LC/MS. The TIC from the LC/MS analysis demonstrates that peptides derived from Y1045, Y1068, Y1114, and Y1173 did not associate with the SH2 affinity column (Figure 8B). Elution of bound peptides from the affinity column and identification by LC/MS as before revealed that peptides derived from EGFR residues Y992, Y1086, Y1101, and Y1148 bound directly to the SH2 domain of *c-src* (Figure 8C). These experiments demonstrate that a specific subset of EGFR receptor *c-src* phosphorylation sites are also ligands for the SH2 domain of *c-src*.

Phosphorylation of the EGFR Autophosphorylation Domain by c-src Enhances Its Binding Affinity for the SH2

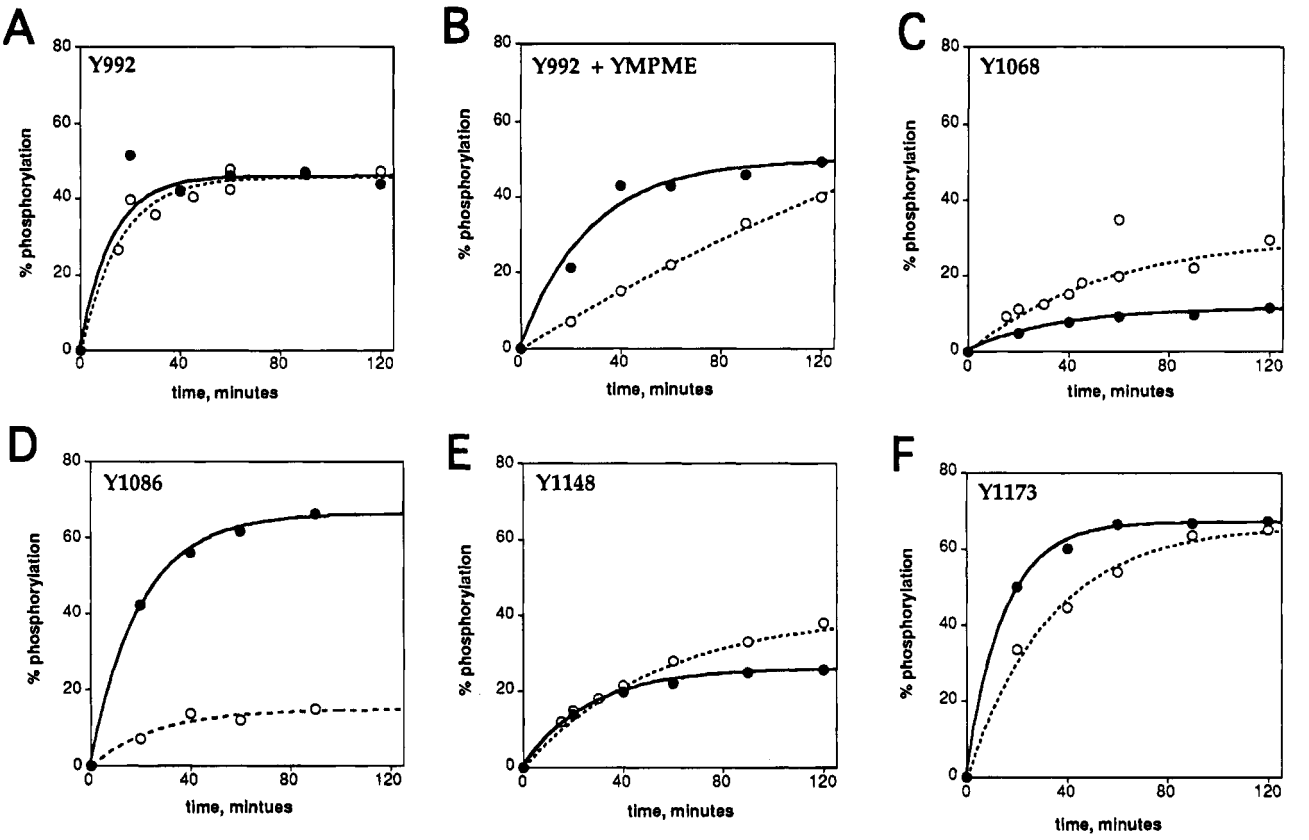

FIGURE 7: Kinetics of site-specific phosphorylation of EGFR. EGFR autophosphorylation domain was phosphorylated by *c-src* (●) or EGFR-KD (○), and samples were taken at the time points indicated in the figures for phosphorylation site mapping. The relative amount of percent phosphorylation as a function of time was calculated by integration of ion current areas corresponding to the tryptic peptide of interest. The curves corresponding to EGFR phosphorylation sites are (A) Y992, (B) Y992 + MEYMPME (sequence of the Glu-Glu epitope tag), (C) Y1068, (D) Y1086, (E) Y1148, and (F) Y1173. The curves were fit to simple first-order kinetics. The single outlying data points in (A), *c-src* for 20 min, and in (C), EGFR-KD for 60 min, were not included in the fit but are shown.

Domain of c-src. Synthetic peptides provide information on the contribution of individual sites that bind to SH2 domains. An extension of such studies is to characterize the effect of multiple site *c-src* phosphorylation of EGFR on its interaction with the SH2 domain of *c-src*. Phosphorylation of EGFR by *c-src* occurs at specific sites that bind directly the SH2 domain of *c-src*. This raised the possibility that covalent modification of EGFR at these sites could have functional consequences with respect to the interaction of EGFR with the *c-src* SH2 domain. The autophosphorylation domain of EGFR was phosphorylated by *c-src* for 60 and 240 min. The direct binding of phosphorylated EGFR to the *c-src* SH2 domain was examined in BIAcore surface plasmon resonance assays (Figure 9B). When the EGFR autophosphorylation domain was phosphorylated for 60 min, the binding to SH2 was characterized by a moderate affinity of 2.5 μM and a Hill coefficient of 1.1 (Figure 9A). In contrast, EGFR that was extensively phosphorylated by *c-src* for 240 min bound to the SH2 domain with a much greater affinity of 380 nM and with a Hill coefficient of 2.0 (Figure 9A). When the data are presented as a Scatchard plot, the concave appearance suggests that when EGFR is extensively phosphorylated by *c-src*, its SH2 domain binding becomes cooperative (Figure 9C). Nonphosphorylated EGFR did not bind to the SH2 domain at concentrations of 6.0 μM (Figure 9A). Collectively, these data suggest that phosphorylation of the EGFR receptor by *c-src* promotes its ability to associate with *c-src* SH2 domains with high affinity and in a cooperative fashion.

DISCUSSION

The studies presented here have defined the *in vitro* sites of *c-src* phosphorylation on the autophosphorylation domain of the EGFR receptor. Furthermore, these tyrosine phosphorylated residues and their accompanying flanking amino acids also constitute ligands for the SH2 domain of *c-src*. These findings are based upon tryptic peptide mapping in conjunction with LC/MS to assign the sites of tyrosine phosphorylation which were similar but not identical to the known autophosphorylation sites of EGFR. *c-src* phosphorylates Y1086 significantly more so than EGFR-KD, while Y1101 is phosphorylated only by *c-src*. These conclusions are also based upon the ability of specific synthetic phosphopeptides derived from sequences surrounding Y992, Y1086, Y1101, and Y1148 to bind directly to the *c-src* SH2 domain in affinity chromatography experiments. In addition, based on BIAcore measurements, extensive phosphorylation of the EGFR autophosphorylation domain by *c-src* results in high-affinity and cooperative binding to the SH2 domain of *c-src*.

The data presented here extend earlier observations that the C-terminal autophosphorylation domain of EGFR serves as an *in vitro* substrate for *c-src* (Koland et al., 1990). The use of mass spectrometry has enabled the sites of phosphorylation by this kinase to be identified readily. The results regarding EGFR tyrosine phosphorylation sites are in agreement with the known *in vivo* autophosphorylation sites. Residues Y992 and Y1173 of the EGFR autophosphorylation

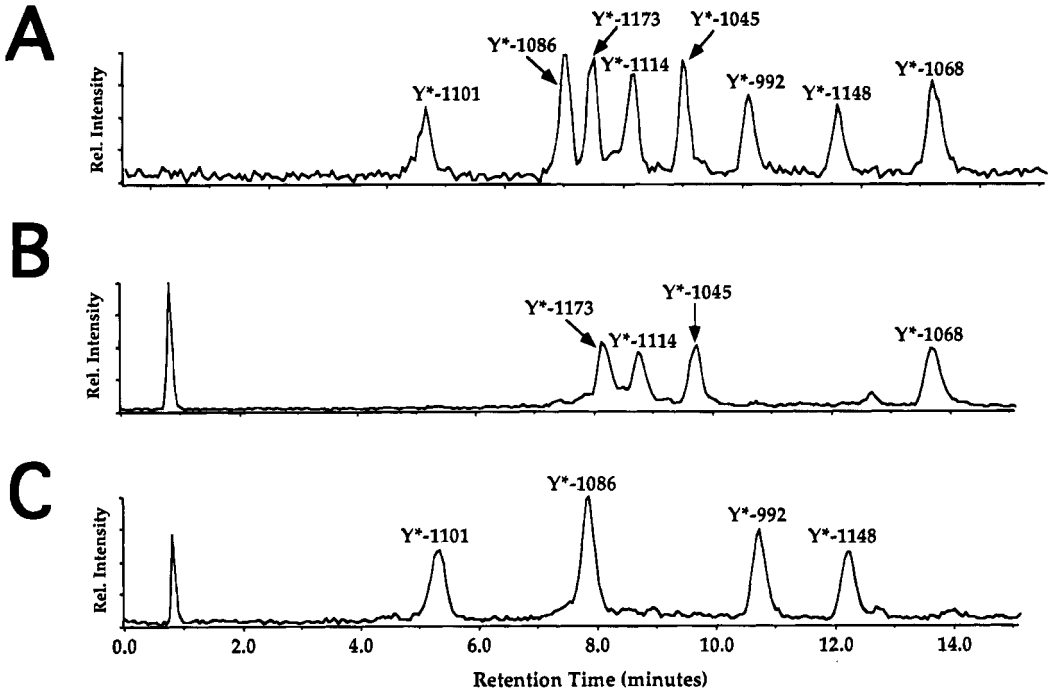

FIGURE 8: TIC of the EGFR phosphopeptides that interact with the *c-src* SH2 domain. An equimolar mixture of synthetic peptides corresponding to the eight potential phosphorylation sites of the EGFR autophosphorylation domain was incubated with a *c-src* SH2 affinity column. The bound and unbound peptides were analyzed by LC/MS as described under Materials and Methods. (A) TIC trace of the eight EGFR phosphopeptide mixture. (B) TIC of the EGFR phosphopeptides not bound to the SH2 column (C) EGFR phosphopeptides that bound to the SH2 affinity column.

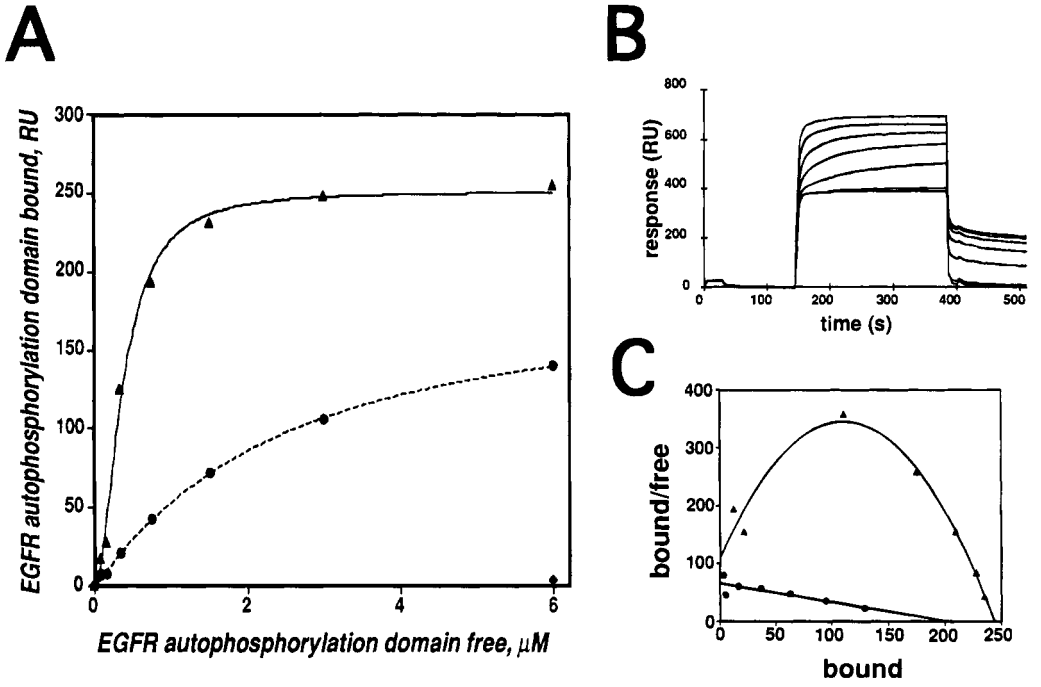

FIGURE 9: Binding of *c-src* phosphorylated EGFR autophosphorylation domain to SH2. (A) EGFR autophosphorylation domain was phosphorylated by *c-src* for 60 min (●) or 240 min (▲) and exchanged by gel filtration into binding buffer. The binding of increasing concentrations (0−6.0 μM) of *s-src*-phosphorylated EGFR to the SH2 domain of *c-src* was measured by BIAcore as described under Materials and Methods. Also shown is the binding of nonphosphorylated EGFR to SH2 at 6.0 μM (♦). (B) Overlay of the SH2 binding sensograms where EGFR was phosphorylated for 240 min. (C) A Scatchard plot of the binding data shown in (A). Controls for nonspecific association included the measurement of phosphorylated EGFR binding to avidin at each concentration tested. These values were less than 10% and were subtracted to give the data shown in (A) and (C).

domain were most rapidly phosphorylated by both kinases (Figure 7), which is consistent with the observation that these sites are the most rapidly and highly autophosphorylated residues during EGFR activation *in vivo* (Downward et al., 1984). The sequences of the preferred phosphorylation sites are specified by acidic amino acids flanking the tyrosine residue and are important for general substrate recognition by tyrosine kinases (Patschinsky et al., 1982). This provides a possible explanation for the observation that *c-src* and EGFR-KD phosphorylate the same sites, the majority of

which contain a glutamic or aspartic acid residue N-terminal to the tyrosine. Interestingly, *c-src* specificity is conferred by a hydrophobic residue at the −1 position (Songyang et al., 1995) which is the case for Y1086 of EGFR (valine at the −1 position). Specific tyrosine residues phosphorylated by *c-src* have been shown to represent phosphotyrosine binding sites for the SH2 domain of *c-src*. Phosphotyrosine binding sites for SH2-containing proteins within the EGFR autophosphorylation domain are not rigorously restricted to a single sequence as is observed for the PDGF receptor (Concepcio et al., 1994). In a previous study, Y992 was identified in coprecipitation assays as a region that associates with the SH2 domain of avian *c-src* (Sierke et al., 1993). The data presented here demonstrate that Y992, Y1148, Y1086, and Y1101 are all capable of this interaction with the SH2 domain of human *c-src* (Figure 8). Furthermore, EGFR phosphopeptides identified here that associate with SH2 domains also competed for SH2−EGFR interactions in ELISA assays (Luttrell et al., 1994). Thus, these studies suggest that the interaction of EGFR with SH2 domains is multivalent and complex or, alternatively, represents a lack of strong sequence specificity in such associations.

The *in vitro* phosphorylation by *c-src* appears to be specific given that not all tyrosine residues are modified. In addition, there are distinct quantitative and qualitative differences between the sites and levels of phosphorylation by the *c-src* vs EGFR-KD activities. For example, Y1086 is weakly phosphorylated by EGFR-KD *in vivo* (Hsuan et al., 1989) and *in vitro* (this report). In contrast, *c-src* phosphorylated this site extensively *in vitro*. Although the percent phosphorylation at Y1101 by *c-src* is lower compared to other sites, this residue has not been identified previously as an EGFR autophosphorylation site. More importantly, there is no known SH2 domain containing protein that associates with this site. A limitation of the present report is that additional putative sites of tyrosine phosphorylation in the EGFR-KD domain and juxtamembrane region cannot be ruled out. A qualitative comparison of EGFR tryptic peptide maps from cell lines overexpressing *v-src* has provided evidence that the sites of *v-src* phosphorylation are distinct from receptor autophosphorylation sites (Wasilenko et al., 1991) and is in reasonable agreement with the findings reported here. This may represent distinctions regarding the substrate specificity of *v-src* versus *c-src* or perhaps reflects real differences in EGFR phosphorylation *in vivo*. Very recently, Stover et al. (1995) provided evidence for *in vivo* phosphorylation of EGFR by *c-src*, including the identification of some phosphorylation sites contained within the EGFR autophosphorylation domain. These observations leave the possibility that the *in vitro c-src* phosphorylation of the autophosphorylation domain of EGFR has potential biological significance.

Biochemical evidence has been presented that EGFR sites of *c-src* phosphorylation represent the preferred binding sites for the *c-src* SH2 domains. This interpretation is consistent with recent results obtained with degenerate peptide libraries where a similar specificity was demonstrated for the Abl and Lck tyrosine kinases (Songyang et al., 1995). The presence of SH2 domains on PLC-γ (Rotin et al., 1992) and *c-src* (Sierke & Koland, 1993) enhances EGFR tyrosine kinase activity toward these proteins. Thus, SH2 domains not only target proteins to receptors but also increase the activity of receptor tyrosine kinases toward these substrates. This apparent enhanced activity of a kinase toward its substrate may be due to an increased local concentration caused by sequestration of the substrate. This raises an interesting hypothesis that the SH2 domain of *c-src* binds to autophosphorylated EGFR and permits cross-phosphorylation of EGFR by *c-src*. The ability of the Y992 phosphopeptide to compete for EGFR−SH2 interactions (Luttrell et al., 1994) suggests that this region of EGFR may bind to *c-src* SH2 with high affinity. It is possible that during receptor autoactivation *c-src* associates initially via its SH2 domain with EGFR at Y992 and subsequently phosphorylates EGFR at other sites, e.g., Y1086 and Y1101. This would create binding sites for additional *c-src* molecules *and/or* SH2-bearing signaling proteins that associate with EGFR. The observation that extensive phosphorylation of EGFR by *c-src* promotes positive cooperativity (Figure 9) in SH2 interactions supports this notion. However, it cannot be ruled out that this apparent cooperativity is an experimental consequence of the combination of immobilization of the SH2 domain on the sensor chip and the multiple sites of phosphorylation on the EGFR autophosphorylation domain. It may be relevant, though, *in vivo* as *c-src* is membrane-associated by virtue of N-myristoylation and EGFR is a membrane-spanning receptor. If such a mechanism were operational *in vivo*, phosphorylation of nearest-neighbor signaling proteins bound to activated EGFR by *c-src* would also be possible. These *in vitro* studies do not completely delineate whether these events do indeed occur *in vivo*. Thus, the biological significance of *c-src* phosphorylation of the EGFR autophosphorylation domain remains undefined. While further studies will be required to resolve these possibilities, an expected outcome of *c-src* phosphorylation would be the attenuation and amplification of the mitogenic signal mediated by EGFR. In support of this hypothesis, overexpression of *c-src* in cells is known to potentiate EGF-activated mitogenesis (Luttrell et al., 1988; Wilson et al., 1989; Wasilenko, 1991), and *c-src* activation is closely linked to the expression levels of EGFR (Osherov & Levitzki, 1994). These experiments identifying the sites of *c-src* phosphorylation on the EGFR autophosphorylation domain as *c-src* SH2 binding sequences support the notion that these interactions play a key role in the biology of mitogenic signal transduction and malignant transformation.

ACKNOWLEDGMENT

Kevin Blackburn is gratefully acknowledged for technical assistance. Will Burkhart and Mary Moyer are gratefully acknowledged for N-terminal amino acid sequencing. Inder Patel and Kelly Lewis are thanked for construction of the EGFR autophosphorylation domain expression plasmid. Martin Rink is acknowledged for expression of the recombinant proteins. Pamela Delacy and Byron Ellis are thanked for purification of *c-src*. Derril Willard is acknowledged for the purification of the SH2−BAD protein. Michael Luther, Tona Gilmer, and Dierdre Luttrell are acknowledged for helpful scientific insights and discussions.

REFERENCES

Biemann, K. (1990) *Methods Enzymol. 193*, 886−887.
Cantley, L., & Songyang, Z. (1994) *J. Cell Sci., Suppl. 18*, 121−126.
Carter, T. H., & Kung, H. J. (1994) *Crit. Rev. Oncog. 5*, 389−428.

Chaiken, I., Rose, S., & Karlsson, R. (1991) *Anal. Biochem. 201*, 197−210.
Concepcio, S.; Beguinot, L., & Carpenter, G. (1994) *J. Biol. Chem. 269*, 12320−12324.
Ding, J., Burkhart, W., & Kassel, D. B. (1994) *Rapid Commun. Mass Spectrom. 8*, 94−98.
Downward, J., Parker, P., & Waterfield, M. D. (1984) *Nature 311*, 483−485.
Ellis, C., Moran, M., McCormick, F., & Pawson, T. (1990) *Nature 343*, 377−381.
Ellis, B., Delacy, P., Weigl, D., Patel, I., Wisely, B., Lewis, K., Overton, L., Cadwell, S., Kost, T., Hoffman, C., Barrett, G., Knight, B., Edison, A., Huang, X., Kassel, D., Berman, J., Rodrigues, M., & Luther, M. (1994) *J. Cell. Biochem. 18B*, 276.
Felder, S., Zhou, M., Hu, P., Urena, J., Ullrich, A., Chaudhuri, M., White, M., Shoelson, S. E., & Schlessinger, J. (1993) *Mol. Cell. Biol. 13*, 1449−1455.
Fry, M. J., Panayotou, G., Booker, G. W., & Waterfield, M. D. (1993) *Protein Sci. 2*, 1785−1797.
Garrett, M. D., Self, A. J., van Oers, C., & Hall, A. (1989) *J. Biol. Chem. 264*, 10−13.
Gregoriou, M., Willis, A. C., Pearson, M. A., & Crawford, C. (1994) *Eur. J. Biochem. 223*, 455−464.
Hsuan, J. J., Totty, N., & Waterfield, M. D. (1989) *Biochem. J. 262*, 659−663.
Huddleston, M. J., Annan, R. S., Bean, M. F., & Carr, S. A. (1993) *J. Am. Soc. Mass Spectrom. 4*, 710−717.
Kassel, D. B., Consler, T. G., Shalaby, M., Sekhri, P., Gordon, N., & Nadler, T. (1995) in *Techniques in Protein Chemistry* (Crabb, J. W., Ed.) pp 39−46, Academic Press, New York.
Koland, J. G., O'Brien, K. M., & Cerione, R. A. (1990) *Biochem. Biophys. Res. Commun. 166*, 90−100.
Lenhard, J. M., Kassel, D. B., Rocque, W. J., Hamacher, L., Holmes, W. D., Patel, I., Hoffman, C., & Luther, M. (1995) *Biochem. J.* (submitted for publication).
Li, N., Schlessinger, J., & Margolis, B. (1994) *Oncogene 9*, 3457−3465.
Lowenstein, E. J., Daly, R. J., Batzer, A. G., Li, W., Margolis, B., Lammers, R., Ullrich, A., Skolnik, E. Y., Bar-Sagi, D., & Schlessinger, J. (1992) *Cell 70*, 431−442.
Luttrell, D. K., Luttrell, L. M., & Parsons, S. J. (1988) *Mol. Cell. Biol. 8*, 497−501.
Luttrell, D. K., Lee, A., Lansing, T. J., Crosby, R. M., Jung, K. D., Willard, D., Luther, M., Rodriguez, M., Berman, J., & Gilmer, T. M. (1994) *Proc. Natl. Acad. Sci. U.S.A. 91*, 83−87.
Mayer, B. J., Hirai, H., & Sakai, R. (1995) *Curr. Biol. 5*, 296−305.
Osherov, N., & Levitzki, A. (1994) *Eur. J. Biochem. 225*, 1047−1053.
Panayotou, G., Bax, B., Gout, I., Federwisch, M., Wroblowski, B., Dhand, R., Fry, M. J., Blundell, T. L., Wollmer, A., & Waterfield, M. D. (1992) *EMBO J. 11*, 4261−4272.
Patschinsky, T., Hunter, T., Esch, F. S., Cooper, J. A., & Sefton, B. M. (1982) *Proc. Natl. Acad. Sci. U.S.A. 79*, 973−977.
Rotin, D., Honegger, A. M., Margolis, B. L., Ullrich, A., & Schlessinger, J. (1992) *J. Biol. Chem. 267*, 9678−9683.
Schlessinger, J. (1994) *Curr. Opin. Genet. Dev. 4*, 25−30.
Settleman, J., Albright, C. F., Foster, L. C., & Weinberg, R. A. (1992) *Nature 359*, 153−154.
Shoelson, S. E., Sivaraja, M., Williams, K. P., Hu, P., Schlessinger, J., & Weiss, M. A. (1993) *EMBO J. 12*, 795−802.
Sierke, S., & Koland, J. G. (1993) *Biochemistry 32*, 10102−10108.
Sierke, S., Longo, G. M., & Koland, J. G. (1993) *Biochem. Biophys. Res. Commun. 191*, 45−54.
Songyang, Z., Shoelson, S. E., Chaudhuri, M., Gish, G., Pawson, T., Haser, W. G., King, F., Roberts, T., Ratnofsky, S., Lechleider, R. J., & et al. (1993) *Cell 72*, 767−778.
Songyang, Z., Shoelson, S. E., McGlade, J., Olivier, P., Pawson, T., Bustelo, X. R., Barbacid, M., Sabe, H., Hanafusa, H., Yi, T., & et al. (1994) *Mol. Cell. Biol. 14*, 2777−2785.
Songyang, Z., Carraway, K. L., III, Eck, M. J., Harrison, S. C., Reldman, R. A., Mohammadi, M., Schessinger, J., Hubbard, S. R., Smith, D. P., Eng, C., Lorenzo, M. J., Ponder, B. A. J., Mayer, B., & Cantley, L. (1995) *Nature 373*, 536−539.
Stover, D. R., Becker, M., Liebetanz, J., & Lydon, N. B. (1995) *J. Biol. Chem. 270*, 15591−15597.
van der Geer, P., Hunter, T., & Lindberg, R. A. (1994) *Annu. Rev. Cell Biol. 10*, 251−337.
Wasilenko, W. J., Payne, D. M., Fitzgerald, D. L., & Weber, M. J. (1991) *Mol. Cell. Biol. 11*, 309−321.
Wedegaertner, P. B., & Gill, G. (1989) *J. Biol. Chem. 264*, 11346−11353.
Wilson, L. K., Luttrell, D. K., Parsons, T., & Parsons, S. J. (1989) *Mol. Cell. Biol. 9*, 1536−1544.
Zhou, M., Felder, S., Rubinstein, M., Hurwitz, D. R., Ullrich, A., Lax, I., & Schessinger, J. (1993) *Biochemistry 32*, 8193−8198.

BI951280B